

A DECOUPLING AND LINEARIZING DISCRETIZATION FOR POROELASTICITY WITH NONLINEAR PERMEABILITY

R. ALTMANN[†], R. MAIER[‡]

ABSTRACT. We analyze a semi-explicit time discretization scheme of first order for poroelasticity with nonlinear permeability provided that the elasticity model and the flow equation are only weakly coupled. The approach leads to a decoupling of the equations and, at the same time, linearizes the nonlinearity without the need of further inner iteration steps. Hence, the computational speed-up is twofold without a loss in the convergence rate. We prove optimal first-order error estimates by considering a related delay system and investigate the method numerically for different examples with various types of nonlinear displacement-permeability relations.

Key words. nonlinear poroelasticity, time discretization, decoupling, linearization

AMS subject classifications. 65M12, 65J15, 76S05

1. INTRODUCTION

Poroelasticity is a consolidation model, which couples a Darcy flow of an incompressible viscous fluid to the linear elastic behavior of the surrounding porous media [Bio41]. The setup is of particular importance for physical applications, e.g., in the field of geomechanics [Zob10], and more recently also found success in connection with medical applications [SEWC12, VCT⁺16]. The poroelastic model relies on an averaging of the pressure and the displacement field on very small volumetric elements and assumes small strains and a quasi-static behavior, i.e., internal equilibria are preserved at any time. In the context of a constant permeability, the model is analyzed in [DC93, Sho00]. However, depending on the particular model configuration, the permeability may depend on the porosity, as, e.g, investigated by Kozeny [Koz27] and Carman [Car37, Car38]. In the context of poroelasticity, the porosity, in turn, depends (in a nonlinear way) on the displacement, which leads to a nonlinear poroelastic model as analyzed in [CCM13] and, in a more general setting, in [BGSW16].

Due to the present nonlinearity, linearization approaches are required to solve the nonlinear system that occurs in every time step of an implicit time discretization. A prominent example is the application of a Picard-type iteration as used, for instance, in [CCM13, BV16, FCM20]. For strong nonlinearities, where multiple inner steps are required, this leads to relatively expensive computations. One important aspect in this context is the coupling of the involved equations. In the context of linear problems, this can be overcome with a suitable decoupling. One approach is the so-called *fixed-stress splitting scheme* considered in [WG07, KTJ11, MW13]. The resulting numerical methods, however, are based on an additional iteration in each time step, see, e.g., [SBK⁺19]. These ideas have also been used in the context of a nonlinear poroelastic model in [BRKN18].

Date: April 21, 2021.

In this contribution, we investigate the use of a semi-explicit time discretization scheme in the setting where the coupling between the two poroelastic equations is rather small; cf. the rigorous condition given in Assumption 2.3. We refer to this particular configuration as *weak coupling*, which is satisfied in many applications. The advantage of a semi-explicit discretization for the classical (linear) poroelastic model was studied in [AMU21a]. Therein it was shown that a semi-explicit Euler discretization maintains the first-order convergence and at the same time decouples the system equations. This decoupling of the flow and the elasticity equations enables a remarkable computational speed-up compared to a classical implicit discretization. In the here considered nonlinear setting, this speed-up is further enhanced by the fact that the semi-explicit discretization naturally leads to a linearization of the nonlinear term, which does not require additional inner iterations to handle the nonlinearity.

Since we are mainly interested in investigating the advantages of using a semi-explicit discretization, we put the theoretical focus on the temporal discretization. This means, in particular, that we present the convergence analysis of the semi-explicit scheme without spatial approximations. Note, however, that the given convergence proof can be extended to the fully discrete setting without further complications.

The remaining parts of the paper are structured as follows. In Section 2, we state the nonlinear poroelasticity model and introduce necessary assumptions. Moreover, several examples of displacement-dependent nonlinear permeabilities are discussed. We then investigate the semi-explicit discretization scheme, leading to (semi-discrete) error estimates in Section 3. For this, we introduce a related delay model, where the time delay equals the step size of the temporal discretization. We then analyze the semi-explicit scheme based on the theoretical observation that it can be reinterpreted as an implicit discretization of the delay model. Finally, we assess the scheme numerically in Section 4, where we consider several nonlinear permeability models.

Notation. Throughout the paper we write $a \lesssim b$ to indicate that there exists a generic constant C , independent of spatial or temporal discretization parameters, such that $a \leq Cb$. Further, we abbreviate Bochner spaces (especially when considering the norms) on the time interval $[0, T]$ for a Banach space \mathcal{X} by $L^p(\mathcal{X}) := L^p(0, T; \mathcal{X})$, $W^{k,p}(\mathcal{X}) := W^{k,p}(0, T; \mathcal{X})$, and $H^k(\mathcal{X}) := H^k(0, T; \mathcal{X})$, $p \geq 1$, $k \in \mathbb{N}$.

2. NONLINEAR POREOELASTICITY

Let $D \subseteq \mathbb{R}^d$, $d \in \{2, 3\}$, be a domain with Lipschitz boundary ∂D . Generally, the poroelastic equations seek the pore pressure $p: [0, T] \times D \rightarrow \mathbb{R}$ and the displacement field $u: [0, T] \times D \rightarrow \mathbb{R}^d$ up to a given final time $T > 0$ such that

$$(2.1a) \quad -\nabla \cdot \sigma(u) + \nabla(\alpha p) = 0 \quad \text{in } (0, T] \times D,$$

$$(2.1b) \quad \partial_t \left(\alpha \nabla \cdot u + \frac{1}{M} p \right) - \nabla \cdot \left(\frac{\kappa(\nabla \cdot u)}{\nu} \nabla p \right) = g \quad \text{in } (0, T] \times D.$$

Here, g is the fluid source and σ denotes the *stress tensor*. The permeability κ is the source of a possible nonlinearity that will be discussed in the following subsections. The remaining constants read α (*Biot-Willis fluid-solid coupling coefficient*), M (*Biot modulus*), and ν (*fluid viscosity*); see [Bio41, Sho00] for further details. For simplicity, we consider homogeneous Dirichlet boundary conditions, i.e.,

$$(2.1c) \quad u = 0 \quad \text{on } (0, T] \times \partial D,$$

$$(2.1d) \quad p = 0 \quad \text{on } (0, T] \times \partial D.$$

More general inhomogeneous boundary conditions may be incorporated in form of a constraint [AMU20]. As initial condition we have $p(\cdot, 0) = p^0$, which also defines $u(\cdot, 0)$ due to (2.1a).

2.1. Linear model and weak form. If the stress-strain constitutive law given by σ is linear and the permeability κ is constant, then system (2.1) is called *linear poroelasticity*. In this case, σ has the form

$$\sigma(u) := 2\mu \varepsilon(u) + \lambda (\nabla \cdot u) \text{id},$$

where μ and λ are the *Lamé coefficients*, id is the identity tensor, and

$$\varepsilon(u) = \frac{1}{2} (\nabla u + (\nabla u)^T)$$

is the *symmetric strain gradient*. Note that the Lamé coefficients may explicitly depend on the spatial variables, causing multiscale effects [BV16, FAC⁺19, ACM⁺20].

In view of the numerical approximation of the solution, we consider the corresponding weak formulation. For this, we introduce the Hilbert spaces

$$\mathcal{V} := [H_0^1(\Omega)]^d, \quad \mathcal{Q} := H_0^1(\Omega)$$

as ansatz spaces for u and p , respectively. Accordingly, we define the two pivot spaces $\mathcal{H}_{\mathcal{V}} := [L^2(\Omega)]^d$ and $\mathcal{H}_{\mathcal{Q}} := L^2(\Omega)$ such that $\mathcal{V}, \mathcal{H}_{\mathcal{V}}, \mathcal{V}^*$ and $\mathcal{Q}, \mathcal{H}_{\mathcal{Q}}, \mathcal{Q}^*$ define Gelfand triples with dense embeddings, see [Zei90, Ch. 23.4]. The L^2 -inner products corresponding to $\mathcal{H}_{\mathcal{V}}$ and $\mathcal{H}_{\mathcal{Q}}$ are simply denoted by (\cdot, \cdot) .

As a second step, we introduce bilinear forms corresponding to the (differential) operators in (2.1). More precisely, we define $a: \mathcal{V} \times \mathcal{V} \rightarrow \mathbb{R}$, $b, c: \mathcal{Q} \times \mathcal{Q} \rightarrow \mathbb{R}$, and $d: \mathcal{V} \times \mathcal{Q} \rightarrow \mathbb{R}$ by

$$\begin{aligned} a(u, v) &:= \int_{\Omega} \sigma(u) : \varepsilon(v) \, dx, & b(p, q) &:= \int_{\Omega} \frac{\kappa}{\nu} \nabla p \cdot \nabla q \, dx, \\ c(p, q) &:= \int_{\Omega} \frac{1}{M} p q \, dx, & d(u, q) &:= \int_{\Omega} \alpha (\nabla \cdot u) q \, dx \end{aligned}$$

for $u, v \in \mathcal{V}$ and $p, q \in \mathcal{Q}$. Then, the weak formulation of system (2.1) seeks abstract functions $u: [0, T] \rightarrow \mathcal{V}$ and $p: [0, T] \rightarrow \mathcal{Q}$ such that

$$(2.2a) \quad a(u, v) - d(v, p) = 0,$$

$$(2.2b) \quad d(\dot{u}, q) + c(\dot{p}, q) + b(p, q) = (g, q).$$

for all test functions $v \in \mathcal{V}$, $q \in \mathcal{Q}$. Results on the unique solvability of the system in terms of a strong solution are shown in [Sho00]. We will discuss the existence of weak solutions in Proposition 2.2 later on.

Remark 2.1. System (2.2) can be interpreted as a coupled system of an elliptic and a parabolic equation such that a spatial discretization yields a coupled system of an algebraic and a differential equation. As a consequence, system (2.2) equals a so-called *partial differential-algebraic equation*. Furthermore, one can show that the poroelastic equations (2.2) have a port-Hamiltonian structure, cf. [AMU20].

2.2. General setting. Before we introduce the displacement-dependent nonlinear permeability, the aim of this subsection is to gather properties of the introduced bilinear forms for the linear case. Further, we discuss the existence of weak solutions and the *weak coupling* assumption.

The bilinear form $a: \mathcal{V} \times \mathcal{V} \rightarrow \mathbb{R}$ contains the linear elasticity model. Thus, by Korn's inequality we know that a is elliptic with a constant c_a that is characterized by μ , cf. [Cia88, Th. 6.3.4]. Further, a is symmetric and bounded in \mathcal{V} . This implies that $\|\cdot\|_a := a(\cdot, \cdot)^{1/2}$ defines a norm, which is equivalent to the \mathcal{V} -norm, namely

$$c_a \|u\|_{\mathcal{V}}^2 \leq \|u\|_a^2 = a(u, u) \leq C_a^2 \|u\|_{\mathcal{V}}^2.$$

Here, C_a denotes the continuity constant of a . Similarly, with a constant and positive permeability κ one has in the linear model that $b: \mathcal{Q} \times \mathcal{Q} \rightarrow \mathbb{R}$ is symmetric, elliptic, and bounded in \mathcal{Q} . The bilinear form $c: \mathcal{Q} \times \mathcal{Q} \rightarrow \mathbb{R}$ equals a scaled variant of the L^2 -inner product. Hence, it is symmetric, elliptic, and bounded in the pivot space $\mathcal{H}_{\mathcal{Q}}$. As a result, $\|\cdot\|_c := c(\cdot, \cdot)^{1/2}$ defines a norm, which is equivalent to the $\mathcal{H}_{\mathcal{Q}}$ -norm.

The bilinear form $d: \mathcal{V} \times \mathcal{Q} \rightarrow \mathbb{R}$ describes the coupling of the elliptic and parabolic part of the poroelastic system. Since we may integrate by parts, there are two continuity estimates, namely

$$d(u, p) \leq C_d \|u\|_{\mathcal{V}} \|p\|_{\mathcal{H}_{\mathcal{Q}}} \quad \text{and} \quad d(u, p) \leq \tilde{C}_d \|u\|_{\mathcal{H}_{\mathcal{V}}} \|p\|_{\mathcal{Q}}.$$

With these assumptions we can prove the following existence result.

Proposition 2.2 (Weak solution for the linear case). *Consider initial data $p^0 \in \mathcal{H}_{\mathcal{Q}}$ and $g \in L^2(0, T; \mathcal{Q}^*)$. Under the above assumptions on the bilinear forms a , b , c , and d , system (2.2) has a unique weak solution*

$$p \in L^2(0, T; \mathcal{Q}) \cap H^1(0, T; \mathcal{Q}^*) \hookrightarrow C([0, T]; \mathcal{H}_{\mathcal{Q}}), \quad u \in L^2(0, T; \mathcal{V}).$$

Proof. To shorten the proof, let $\mathcal{A}: \mathcal{V} \rightarrow \mathcal{V}^*$, $\mathcal{B}, \mathcal{C}: \mathcal{Q} \rightarrow \mathcal{Q}^*$, and $\mathcal{D}: \mathcal{V} \rightarrow \mathcal{Q}^*$ denote the operators corresponding to the bilinear forms a , b , c , and d , respectively. With this, system (2.2) can equivalently be written in the form

$$\mathcal{A}u - \mathcal{D}^*p = 0 \quad \text{in } \mathcal{V}^*, \quad \mathcal{D}\dot{u} + \mathcal{C}\dot{p} + \mathcal{B}p = g \quad \text{in } \mathcal{Q}^*.$$

Since \mathcal{A} is invertible, we can (formally) differentiate the first equation in time and insert it into the second. This then yields the equation

$$(\mathcal{C} + \mathcal{D}\mathcal{A}^{-1}\mathcal{D}^*)\dot{p} + \mathcal{B}p = g.$$

It remains to show that this is a (linear) parabolic equation, which then implies the existence of a unique solution $p \in L^2(0, T; \mathcal{Q})$ with $\dot{p} \in L^2(0, T; \mathcal{Q}^*)$; cf. [LM72, Ch. 3, Sect. 4]. Moreover, by the first equation, we conclude the existence of u . The second equation, in turn, shows that $\mathcal{D}\dot{u} \in L^2(0, T; \mathcal{Q}^*)$.

By assumption, we know that \mathcal{B} is elliptic. We show that $\tilde{\mathcal{C}} := \mathcal{C} + \mathcal{D}\mathcal{A}^{-1}\mathcal{D}^*$ defines an inner product in $\mathcal{H}_{\mathcal{Q}}$. Since \mathcal{C} is assumed to be elliptic, it is sufficient to note that for $p \in \mathcal{H}_{\mathcal{Q}}$ we have $\langle \mathcal{D}\mathcal{A}^{-1}\mathcal{D}^*p, p \rangle = \langle \mathcal{A}^{-1}\mathcal{D}^*p, \mathcal{D}^*p \rangle \geq 0$. \square

For the convergence analysis of Section 3 we need the assumption that the coupling is sufficiently weak in the following sense.

Assumption 2.3 (weak coupling condition). We assume a weak coupling of the form

$$C_d^2 \leq c_a c_c,$$

where c_a, c_c denote the ellipticity constants of the bilinear forms a, c , respectively, and C_d the continuity constant of d .

Remark 2.4. In the field of poroelasticity, the coefficient α (and thus C_d) is often bounded by 1. Note that this is several magnitudes smaller than the typical Lamé coefficients, cf. [DC93, Sect. 3.3.4]. As a result, Assumption 2.3 is satisfied in many applications as they appear, e.g., in the field of geomechanics.

In the following, we discuss a nonlinear extension of the poroelastic equations, where we allow the bilinear form b to depend on the displacement.

2.3. Nonlinear displacement-dependent permeability. We now leave the linear setting and assume that the permeability κ depends (in a possibly nonlinear fashion) on the divergence of the displacement. Thus, we replace the previously defined bilinear form b by

$$(2.3) \quad b(u; p, q) := \int_{\Omega} \frac{\kappa(\nabla \cdot u)}{\nu} \nabla p \cdot \nabla q \, dx.$$

Note that for fixed u , b has the same structure as in the linear case. Here, however, we consider the nonlinear case, which leads to the system

$$(2.4a) \quad a(u, v) - d(v, p) = 0,$$

$$(2.4b) \quad d(\dot{u}, q) + c(\dot{p}, q) + b(u; p, q) = (g, q)$$

for test functions $v \in \mathcal{V}$, $q \in \mathcal{Q}$ and with the initial condition $p(0) = p^0$. For the nonlinearity, we make the following assumptions.

Assumption 2.5 (nonlinear permeability). We assume that κ is Lipschitz continuous and bounded in terms of constants κ_- and κ_+ , i.e.,

$$(2.5) \quad 0 < \kappa_- \leq \kappa \leq \kappa_+ < \infty.$$

This implies the existence of a positive constant L_b (depending on ν , κ_+ , and the Lipschitz constant of κ) such that $b: \mathcal{V} \times \mathcal{Q} \times \mathcal{Q} \rightarrow \mathbb{R}$ introduced in (2.3) satisfies

$$(2.6a) \quad \|b(u; p, \cdot) - b(u; q, \cdot)\|_{\mathcal{Q}^*} \leq L_b \|p - q\|_{\mathcal{Q}},$$

$$(2.6b) \quad \|b(u; p, \cdot) - b(v; p, \cdot)\|_{\mathcal{Q}^*} \leq L_b \|p\|_{\mathcal{Q}} \|u - v\|_{\mathcal{V}}$$

for all $u, v \in \mathcal{V}$ and $p, q \in \mathcal{Q}$. Furthermore, the lower bound of κ yields

$$(2.7) \quad b(u; p, p) \geq c_b \|p\|_{\mathcal{Q}}^2$$

uniformly in $u \in \mathcal{V}$ and for all $p \in \mathcal{Q}$, where c_b depends on ν and κ_- .

We emphasize that the remaining bilinear forms a , c , and d remain unchanged, i.e., we keep the assumptions from Section 2.1. Further note that Assumption 2.5 is a generalization of the linear case presented in Section 2.1, since the assumptions simplify to the continuity and ellipticity of the operator in the constant case $\kappa(\nabla \cdot u) \equiv \kappa$.

In the outlined setting, we can conclude the solvability of the nonlinear poroelasticity problem. Uniqueness is discussed afterwards.

Proposition 2.6 (Solvability of the nonlinear system). *Consider the setting from Section 2.1 with b defined in (2.3) satisfying Assumption 2.5. Further, let the initial data satisfy $p^0 \in \mathcal{H}_{\mathcal{Q}}$ and $g \in L^2(0, T; \mathcal{H}_{\mathcal{Q}})$. Then, system (2.4) contains a weak solution*

$$u \in L^2(0, T; \mathcal{V}), \quad p \in L^2(0, T; \mathcal{Q}).$$

Proof. The existence of a solution has been shown in [CCM13, Th. 2.9] for the slightly more general case of κ being continuous rather than Lipschitz continuous. The proof is based on the fact that, given $p \in \mathcal{H}_Q$, equation (2.4a) yields a unique $u \in \mathcal{V}$. Thus, the variable u can be eliminated. Afterwards, the existence of a solution is shown by a Rothe discretization, i.e., a discretization first in time and then in space. \square

Remark 2.7 (Uniqueness of solutions). The uniqueness of a solution to (2.4) is investigated in [CCM13, Th. 2.10] and requires additional assumptions such as the Lipschitz continuity of κ . Further, it is asked for a condition, which is similar to our weak coupling condition stated in Assumption 2.3. Translated to our notion, the sufficient condition reads

$$C_d^2 (C_P^2 \tilde{C}_P \frac{\kappa_+}{\kappa_-}) < c_a c_c,$$

where C_P and \tilde{C}_P are the constants in the Poincaré-type estimates $\|v\|_{\mathcal{H}_V} \leq \tilde{C}_P \|\nabla \cdot v\|_{\mathcal{H}_V}$ and $\|q\|_Q \leq C_P \|\nabla q\|_{\mathcal{H}_V}$ for $v \in \mathcal{V}$, $q \in \mathcal{Q}$. Hence, we recover the weak coupling condition up to a constant factor, which depends on κ . The final condition for the unique solvability of (2.4) is an L^∞ -bound of ∇p , which can be achieved considering sufficiently smooth data.

In the remainder of this paper, we will always assume the existence of a unique solution (u, p) to (2.4) and concentrate on the numerical approximation of this solution.

2.4. Particular choices of the displacement-dependence in the permeability. To understand the explicit dependence of the permeability κ on the divergence of the displacement, we emphasize that in many interesting configurations, the permeability may be assumed to depend on the *porosity*, which describes the volume fraction which is occupied by the fluid. A well-established and in many cases reliable hypothesis for the explicit dependence on the porosity is the so-called *Kozeny-Carman* relation, which traces back to Kozeny [Koz27] and was later on adjusted by Carman [Car37, Car38]. It couples the permeability in a nonlinear fashion to the porosity. For the particular case of a flow of a Newtonian fluid in the interstice between spherical particles in the context of poroelasticity, such a behavior is used and justified in [HC90]. The relation is further applied in [KP99] to derive a permeability-displacement dependence under the assumption that the solid grains are relatively incompressible compared to the solid skeleton of the porous medium. To achieve this, a relation of the porosity and the *volume strain* or *dilatation* is required. The dilatation expresses the change of volume of the fluid and (under the assumption of small strains) is given by $\nabla \cdot u$. This explains the specific form of the permeability given in (2.3), which is considered throughout this work.

A particular model for the permeability-displacement relation, which includes the Kozeny-Carman relation, is presented in the following example.

Example 2.8 (Kozeny-Carman-type permeability). A prominent case of a displacement-dependent permeability through the dilatation is the above-mentioned Kozeny-Carman-type permeability as considered in [CCM13, BGSW16] in the context of a poroelastic problem with linear stress-strain relations. The particular choice of κ used therein reads

$$\kappa(s) := \begin{cases} \kappa_-, & s \leq c_s, \\ \kappa_0 \frac{\rho^3(s)}{(1 - \rho(s))^2}, & c_s < s < C_s, \\ \kappa_+, & s \geq C_s, \end{cases}$$

where κ_0 is the initial saturated permeability and ρ the porosity, i.e., the ratio between fluid volume and total volume given by

$$\rho(s) = \rho_0 + (1 - \rho_0)s,$$

where $\rho_0 \in (0, 1)$ is a given ground porosity. Further, c_s and C_s are some prescribed lower and upper bounds which fulfill

$$\frac{\rho_0}{\rho_0 - 1} < c_s < C_s < 1$$

and lead to

$$\kappa_- = \kappa_0 \frac{\rho^3(c_s)}{(1 - \rho(c_s))^2}, \quad \kappa_+ = \kappa_0 \frac{\rho^3(C_s)}{(1 - \rho(C_s))^2}.$$

We emphasize that this particular example satisfies Assumption 2.5 due to the explicit bounds and the Lipschitz continuity of κ .

Apart from the presented Kozeny-Carman relation, also other representations of the permeability exist, which might depend on the geometrical setup or the specific problem configuration. Another coupling of porosity and permeability is, for instance, considered in [CGH⁺14] to model blood flow in the lamina cribrosa. Therein, the permeability depends quadratically on the dilatation, which turns out to be suitable to describe the flow of a Newtonian fluid through cylindrical pores. Finally, we also mention the *network-inspired* permeability as described in [RLVM20] and the exponential dependence on the displacement as investigated in [LM80, HM90], again in the context of biological tissues.

The network-inspired model is described in the following example with an artificially introduced lower bound to fulfill Assumption 2.5.

Example 2.9 (Network-inspired permeability). In network structures consisting of channels that can be open or closed, the flow rate depends on the number of channels that are open, see, e.g. [Bal87, Won88]. Considering the possibility of channels being randomly closed or open, a permeability-porosity relation is presented in [RLVM20] for an arbitrary network topology that reads

$$\hat{\kappa}(s) := \begin{cases} 0, & \rho(s) < \hat{\rho}, \\ \kappa_0 \frac{\rho(s) - \hat{\rho}}{\rho_0 - \hat{\rho}}, & \rho(s) \geq \hat{\rho}, \end{cases}$$

where the porosity ρ is given by

$$\rho(s) = 1 - (1 - \rho_0) \exp(-s)$$

with $\rho_0, \hat{\rho} \in (0, 1)$ and $\hat{\rho} < \rho_0$. In order to fulfill the lower bound in Assumption 2.5, we artificially introduce a threshold in the permeability and define

$$\kappa(s) = \hat{\kappa}(s) + \kappa_0 \delta$$

with some small $\delta > 0$. This ensures that a flow through the medium is always possible.

Remark 2.10 (Nonlinear thermoelasticity). Besides the here considered poroelasticity models, the given framework also fits to problems in the field of thermoelasticity, which covers the displacement of a material due to temperature changes. Since linear poroelasticity and linear thermoelasticity are equivalent from a mathematical point of view [Bio56], the given setting also includes applications with a nonlinear heat conductivity. Note that, in order to satisfy Assumption 2.3, the thermal expansion coefficient needs to be much smaller than the stress tensor, cf. [CR14].

3. TIME DISCRETIZATION

This section is devoted to the temporal discretization of the nonlinear system (2.4) by a semi-explicit Euler scheme. We prove first-order convergence under the weak coupling condition of Assumption 2.3. The proposed approach decouples the system, which means that the two equations can be solved sequentially. At the same time, the system is automatically linearized such that no nonlinear solver is needed, leading to a remarkable boost of efficiency.

Throughout this section, we consider an equidistant partition $0 = t_0 < t_1 < \dots < t_N = T$ with step size τ , i.e., $t_n = n\tau$. For simplicity, we assume continuity of g , i.e., $g \in C([0, T]; \mathcal{H}_Q)$, and define $g^n := g(t_n) \in \mathcal{H}_Q$. Note, however, that point evaluations may also be replaced by integral means if the right-hand side is only square-integrable. Accordingly, we assume continuity of the solution pair (u, p) and initial data $p^0 \in \mathcal{Q}$.

Before considering the semi-explicit approach, we shortly discuss the standard approach of a fully implicit Euler discretization applied to (2.4). This leads to the semi-discrete system

$$(3.1a) \quad a(u^n, v) - d(v, p^n) = 0,$$

$$(3.1b) \quad d(D_\tau u^n, q) + c(D_\tau p^n, q) + b(u^n; p^n, q) = (g^n, q)$$

for test functions $v \in \mathcal{V}$, $q \in \mathcal{Q}$. Here, $D_\tau u^n := \tau^{-1}(u^n - u^{n-1})$ denotes the discrete time derivative. The solvability of (3.1) has been discussed in [CCM13, Lem. 2.4], i.e., given $u^{n-1} \in \mathcal{V}$ and $p^{n-1} \in \mathcal{Q}$, there exist $u^n \in \mathcal{V}$ and $p^n \in \mathcal{Q}$ that solve (3.1).

Note that (3.1) still marks a nonlinear system, which needs to be solved in every time step. Thus, a nonlinear solver which comprises an inner iteration is needed. Standard choices implement a Picard iteration, cf. [CCM13, BV16, FCM20]. This is a fixed point iteration and has the following form: Given $u^{n-1} \in \mathcal{V}$, $p^{n-1} \in \mathcal{Q}$ as approximation at time t_{n-1} , we first define $u_0^n := u^{n-1}$ and $p_0^n := p^{n-1}$. Then, we solve for $j = 1, 2, \dots$ the *linear* system

$$(3.2a) \quad a(u_j^n, v) - d(v, p_j^n) = 0,$$

$$(3.2b) \quad \tau^{-1}d(u_j^n - u^{n-1}, q) + \tau^{-1}c(p_j^n - p^{n-1}, q) + b(u_{j-1}^n; p_j^n, q) = (g^n, q)$$

for all $v \in \mathcal{V}$, $q \in \mathcal{Q}$. Obviously, a fixed point satisfies the nonlinear system (3.1). In practice, one defines $u^n := u_j^n$ and $p^n := p_j^n$ for some index j , depending on a certain stopping criterion, e.g., the residual of the current iteration. For corresponding numerical tests we refer to Section 4.2.

3.1. Semi-explicit Euler scheme. We turn to the semi-explicit approach and consider the equidistant partition with step size τ as before. Given the previous iterates $u^{n-1} \in \mathcal{V}$ and $p^{n-1} \in \mathcal{Q}$, we now aim to solve the system

$$(3.3a) \quad a(u^n, v) - d(v, p^{n-1}) = 0,$$

$$(3.3b) \quad d(D_\tau u^n, q) + c(D_\tau p^n, q) + b(u^n; p^n, q) = (g^n, q)$$

for all $v \in \mathcal{V}$, $q \in \mathcal{Q}$. In order to be well-posed, we need to discuss the solvability of system (3.3), which turns out to be much more straightforward than in the fully implicit case.

Lemma 3.1 (Well-posedness of the semi-explicit scheme (3.3)). *Consider the setting from Section 2.1 with b defined in (2.3) satisfying Assumption 2.5. Further assume $u^{n-1} \in \mathcal{V}$, $p^{n-1} \in \mathcal{Q}$, and $g^n \in \mathcal{H}_{\mathcal{Q}}$. Then, system (3.3) attains a unique solution $u^n \in \mathcal{V}$ and $p^n \in \mathcal{Q}$.*

Proof. For fixed p^{n-1} , the term $d(\cdot, p^{n-1})$ defines a functional in \mathcal{V}^* . Thus, by the assumptions on the bilinear form a , equation (3.3a) provides a unique $u^n \in \mathcal{V}$. With this in hand, equation (3.3b) can be rewritten as the *linear* variational problem

$$\tilde{b}(p^n, q) = (\tilde{g}^n, q) := (g^n, q) + \tau^{-1} c(p^{n-1}, q) - \tau^{-1} d(u^n - u^{n-1}, q)$$

with $\tilde{b}(p^n, q) := b(u^n; p^n, q) + \tau^{-1} c(p^n, q)$. The right-hand side satisfies $\tilde{g}^n \in \mathcal{H}_{\mathcal{Q}}$ and the form $\tilde{b}: \mathcal{Q} \times \mathcal{Q} \rightarrow \mathbb{R}$ is elliptic, since

$$\tilde{b}(p, p) = b(u^n; p, p) + \tau^{-1} c(p, p) \geq c_b \|p\|_{\mathcal{Q}}^2.$$

Hence, there exists a unique $p^n \in \mathcal{Q}$, which completes the proof. \square

In order to prove convergence of the semi-explicit scheme, we follow the idea first presented in [AMU21a] for the linear case and consider a delay system, which is closely related to the original system (2.4). This is the subject of the following subsection.

3.2. A related delay system. As an alternative point of view, one may regard the semi-explicit scheme (3.3) as the *implicit* Euler method applied to the delay system

$$(3.4a) \quad a(\bar{u}, v) - d(v, \bar{p}(\cdot - \tau)) = 0,$$

$$(3.4b) \quad d(\dot{\bar{u}}, q) + c(\dot{\bar{p}}, q) + b(\bar{u}; \bar{p}, q) = (g, q)$$

for test functions $v \in \mathcal{V}$ and $q \in \mathcal{Q}$. Note that the time delay is exactly the temporal step size τ and hence fixed. For such a delay system, one needs a prescribed *history function* for \bar{p} in $[-\tau, 0]$ rather than only an initial value. Since there is some freedom of choice regarding the history function, we set $\bar{p}|_{[-\tau, 0]}(t) = \Phi(t)$ and demand

$$(3.5) \quad \Phi(-\tau) = \Phi(0) = p^0, \quad \Phi \in C^\infty([-\tau, 0]; \mathcal{Q}).$$

Note that one particular choice is given by $\Phi \equiv p^0$. In any case, a history function satisfying (3.5) implies $\bar{p}(0) = \Phi(0) = p^0$ and by equation (3.4a) we conclude $\bar{u}(0) = u(0)$, since

$$a(\bar{u}(0), v) = d(v, \Phi(-\tau)) = d(v, p^0).$$

Remark 3.2 (Solvability of the delay system). Assuming sufficient regularity of the right-hand side g and the history function Φ , one can prove the unique solvability of (3.4). For this, one can apply Bellmann's method of steps [BZ03, Ch. 3.4], which considers the intervals $[t_n, t_{n+1}]$ for $n = 0, \dots, N-1$ successively. On the first interval $[0, \tau]$, for example, this gives the parabolic equation

$$c(\dot{\bar{p}}, q) + b_0(\bar{p}, q) = (\tilde{g}, q)$$

for all $q \in \mathcal{Q}$ with (using the operator notation from the proof of Proposition 2.2)

$$\tilde{g} := g - \mathcal{D}\mathcal{A}^{-1}\mathcal{D}^*\dot{\Phi}(\cdot - \tau), \quad b_0(p, q) := \int_{\Omega} \frac{\kappa(\nabla \cdot \mathcal{A}^{-1}\mathcal{D}^*\Phi(\cdot - \tau))}{\nu} \nabla p \cdot \nabla q \, dx.$$

Note that $b_0: \mathcal{Q} \times \mathcal{Q} \rightarrow \mathbb{R}$ is linear, bounded, and (uniformly) elliptic such that [Wlo92, Th. 26.1] is applicable.

In order to use the interpretation of the semi-explicit discretization as an implicit discretization of the corresponding delay system, we need to show that the two systems (2.4) and (3.4) only differ by a term of order τ . To show this, we need the following regularity assumption.

Assumption 3.3. Given $p^0 \in \mathcal{Q}$ and a history function Φ as in (3.5), let systems (2.4) and (3.4) be uniquely solvable. Further assume that the solutions are bounded in the sense that

$$p \in L^\infty(0, T; \mathcal{Q}) \quad \text{and} \quad \bar{p} \in W^2(0, T; \mathcal{H}_\mathcal{Q}).$$

The estimate of the differences $\bar{p} - p$ and $\bar{u} - u$ is subject to the following proposition.

Proposition 3.4 (Difference of original and delay system). *Within the setting of Section 2.1 with b defined in (2.3) satisfying Assumption 2.5, let (u, p) denote the solution to (2.4) with $p(0) = p^0 \in \mathcal{Q}$ and (\bar{u}, \bar{p}) the solution to (3.4) for a history function satisfying (3.5). Then, given Assumption 3.3, we have the error bound*

$$\|\bar{u}(t) - u(t)\|_{\mathcal{V}}^2 + \|\bar{p}(t) - p(t)\|_{\mathcal{H}_\mathcal{Q}}^2 + \int_0^t \|\bar{p}(s) - p(s)\|_{\mathcal{Q}}^2 ds \lesssim \tau^2 (1 + t) \exp(Ct),$$

where the hidden constant depends on $\|\bar{p}\|_{W^{2,\infty}(\mathcal{H}_\mathcal{Q})}$ and the stability and continuity constants of the involved forms a, b, c, d . Further, the constant in the exponential term is given by $C := 2\frac{C_d}{c_a} + 2\frac{L_b^2}{c_a c_b} \|p\|_{L^\infty(\mathcal{Q})}^2$.

Proof. Let us introduce the differences $e_u := \bar{u} - u$ and $e_p := \bar{p} - p$ for which we know that $e_u(0) = 0$ and $e_p(0) = 0$ by the construction of the history function. Next, we consider a Taylor expansion of \bar{p} , namely

$$(3.6) \quad \bar{p}(t - \tau) = \bar{p}(t) - \tau \dot{\bar{p}}(\xi_t)$$

for some $\xi_t \in (t - \tau, t) \subseteq (-\tau, T]$. With this, we can derive

$$(3.7a) \quad a(e_u, v) - d(v, e_p) = -\tau d(v, \dot{\bar{p}}(\xi_t)),$$

$$(3.7b) \quad d(\dot{e}_u, q) + c(\dot{e}_p, q) + b(\bar{u}; \bar{p}, q) - b(u; p, q) = 0$$

for all test functions $v \in \mathcal{V}$, $q \in \mathcal{Q}$. Summing up (3.7a) and (3.7b) with test functions $v = \dot{e}_u$ and $q = e_p$, we obtain

$$a(e_u, \dot{e}_u) + c(\dot{e}_p, e_p) + b(\bar{u}; \bar{p}, e_p) - b(u; p, e_p) = -\tau d(\dot{e}_u, \dot{\bar{p}}(\xi_t))$$

and thus

$$\frac{1}{2} \frac{d}{dt} \|e_u\|_a^2 + \frac{1}{2} \frac{d}{dt} \|e_p\|_c^2 + b(\bar{u}; e_p, e_p) = -\tau d(\dot{e}_u, \dot{\bar{p}}(\xi_t)) - b(\bar{u}; p, e_p) + b(u; p, e_p).$$

Integration over $[0, t]$ and a multiplication by 2 yields

$$\begin{aligned} \|e_u(t)\|_a^2 + \|e_p(t)\|_c^2 + 2 \int_0^t b(\bar{u}; e_p, e_p) ds \\ = -2\tau \int_0^t \int_\Omega \alpha (\nabla \cdot \dot{e}_u) \dot{\bar{p}}(\xi_s) dx ds - 2 \int_0^t b(\bar{u}; p, e_p) - b(u; p, e_p) ds \\ = 2\tau \int_0^t \int_\Omega \alpha (\nabla \cdot e_u) \frac{d}{ds} (\dot{\bar{p}}(\xi_s)) dx ds - 2\tau \int_\Omega \alpha (\nabla \cdot e_u(t)) \dot{\bar{p}}(\xi_t) dx \\ - 2 \int_0^t b(\bar{u}; p, e_p) - b(u; p, e_p) ds, \end{aligned}$$

where we use integration by parts in the last step. For the derivative of $\dot{\bar{p}}(\xi_s)$ we now use the fact that

$$\frac{d}{ds} \dot{\bar{p}}(\xi_s) = \frac{\dot{\bar{p}}(s) - \dot{\bar{p}}(s-\tau)}{\tau} = \ddot{\bar{p}}(\zeta_s)$$

with some new $\zeta_s \in (s - \tau, s) \subseteq (-\tau, T]$. By the ellipticity of b we conclude that

$$\begin{aligned} \|e_u(t)\|_a^2 + \|e_p(t)\|_c^2 + 2c_b \int_0^t \|e_p\|_{\mathcal{Q}}^2 ds \\ \leq 2\tau \int_0^t d(e_u, \ddot{\bar{p}}(\zeta_s)) ds - 2\tau d(e_u(t), \dot{\bar{p}}(\xi_t)) - 2 \int_0^t b(\bar{u}; p, e_p) - b(u; p, e_p) ds. \end{aligned}$$

By Assumption 2.5 we have

$$b(\bar{u}; p, e_p) - b(u; p, e_p) \leq L_b \|p\|_{\mathcal{Q}} \|e_u\|_{\mathcal{V}} \|e_p\|_{\mathcal{Q}}$$

and thus, multiple applications of the weighed Young's inequality [Eva98, App. B] yield

$$\begin{aligned} \|e_u(t)\|_a^2 + \|e_p(t)\|_c^2 + 2c_b \int_0^t \|e_p\|_{\mathcal{Q}}^2 ds \\ \leq C_d \tau^2 t \|\ddot{\bar{p}}\|_{L^\infty(\mathcal{H}_{\mathcal{Q}})}^2 + C_d \int_0^t \|e_u\|_{\mathcal{V}}^2 ds + 2 \frac{C_d^2}{c_a} \tau^2 \|\dot{\bar{p}}\|_{L^\infty(\mathcal{H}_{\mathcal{Q}})}^2 \\ + \frac{1}{2} \|e_u(t)\|_a^2 + c_b \int_0^t \|e_p\|_{\mathcal{Q}}^2 ds + \frac{L_b^2}{c_b} \|p\|_{L^\infty(\mathcal{Q})}^2 \int_0^t \|e_u\|_{\mathcal{V}}^2 ds. \end{aligned}$$

We can now absorb the first two terms in the last line to get

$$\frac{1}{2} \|e_u(t)\|_a^2 + \|e_p(t)\|_c^2 + c_b \int_0^t \|e_p\|_{\mathcal{Q}}^2 ds \leq \tau^2 (C_1 + C_2 t) + C_3 \int_0^t \frac{1}{2} \|e_u\|_a^2 ds$$

with constants $C_1 := 2 \frac{C_d^2}{c_a} \|\dot{\bar{p}}\|_{L^\infty(\mathcal{H}_{\mathcal{Q}})}^2$, $C_2 := C_d \|\ddot{\bar{p}}\|_{L^\infty(\mathcal{H}_{\mathcal{Q}})}^2$, and $C_3 := 2 \frac{C_d}{c_a} + 2 \frac{L_b^2}{c_a c_b} \|p\|_{L^\infty(\mathcal{Q})}^2$. Hence, an application of Grönwall's inequality yields

$$\frac{1}{2} \|e_u(t)\|_a^2 + \|e_p(t)\|_c^2 + c_b \int_0^t \|e_p\|_{\mathcal{Q}}^2 ds \leq \tau^2 (C_1 + C_2 t) \exp(t C_3),$$

which completes the proof. \square

3.3. Proof of convergence. After we have seen that the pairs (u, p) and (\bar{u}, \bar{p}) only differ by a term of order τ , we now analyze the error caused by the *implicit* discretization of the delay system (3.4). For this, we assume that the weak coupling condition introduced in Section 2.2 holds.

Proposition 3.5 (Semi-discrete error for the delay system). *Consider once more the assumptions of Proposition 3.4 including Assumptions 2.5 and 3.3. Further consider the weak coupling condition from Assumption 2.3 as well as*

$$(3.8) \quad \tau < \frac{c_a c_b}{2 L_b^2 \|\bar{p}\|_{L^\infty(\mathcal{Q})}^2}.$$

Let (\bar{u}, \bar{p}) denote the exact solution to (3.4) and (u^n, p^n) the sequence resulting from (3.3) for $n \leq T/\tau$ and exact initial data. Then we have the error bounds

$$\|\bar{u}(t_n) - u^n\|_{\mathcal{V}}^2 + \|\bar{p}(t_n) - p^n\|_{\mathcal{H}_{\mathcal{Q}}}^2 \lesssim \tau^2 (\exp(C t_n) - 1)$$

and

$$\sum_{k=1}^n \tau \|\bar{p}(t_k) - p^k\|_{\mathcal{Q}}^2 \lesssim \tau^2 t_n \exp(C t_n).$$

Here, the hidden constants depend on $\|\bar{p}\|_{W^{2,\infty}(\mathcal{H}_{\mathcal{Q}})}$, $\|\bar{u}\|_{W^{2,\infty}(\mathcal{H}_{\mathcal{V}})}$, and all stability and continuity constants. The constant in the exponential term reads $C := \frac{2L_b^2}{c_a c_b} \|\bar{p}\|_{L^\infty(\mathcal{Q})}^2$.

Remark 3.6. The step size restriction (3.8) is solely dependent on the problem at hand. In particular, this condition is *not* a CFL-type condition that would couple τ to underlying spatial discretization parameters.

Proof of Proposition 3.5. The proof is based on [AMU21a] and follows the ideas of [EM09]. We set

$$\eta_u^n := \bar{u}^n - u^n \in \mathcal{V} \quad \text{and} \quad \eta_p^n := \bar{p}^n - p^n \in \mathcal{Q}$$

as well as

$$\theta_u^{n+1} := \bar{u}^{n+1} - \bar{u}^n - \tau \dot{u}^{n+1} \in \mathcal{V} \quad \text{and} \quad \theta_p^{n+1} := \bar{p}^{n+1} - \bar{p}^n - \tau \dot{p}^{n+1} \in \mathcal{Q},$$

where $\bar{u}^n := \bar{u}(t_n)$ and $\bar{p}^n := \bar{p}(t_n)$ are the (pointwise) solutions of (3.4) and (u^n, p^n) the discrete solution of (3.3) at time point $t_n = \tau n$. By the assumption on the initial data, we have $\eta_u^0 = 0$ and $\eta_p^0 = 0$. Using (3.3a) and (3.4a), we immediately obtain

$$(3.9) \quad \begin{aligned} a(\eta_u^{n+1}, v) - d(v, \eta_p^{n+1}) &= a(\bar{u}^{n+1} - u^{n+1}, v) - d(v, \bar{p}^n - p^n) - d(v, \eta_p^{n+1} - \eta_p^n) \\ &= -d(v, \eta_p^{n+1} - \eta_p^n) \end{aligned}$$

for all $v \in \mathcal{V}$. Further, it holds that

$$(3.10) \quad \begin{aligned} \tau b(u^{n+1}; \eta_p^{n+1}, q) &= \tau b(\bar{u}^{n+1}; \bar{p}^{n+1}, q) - \tau b(u^{n+1}; p^{n+1}, q) \\ &\quad + \tau [b(u^{n+1}; \bar{p}^{n+1}, q) - b(\bar{u}^{n+1}; \bar{p}^{n+1}, q)] \end{aligned}$$

for all $q \in \mathcal{Q}$. With (3.3b), (3.4b), and (3.10), we have that

$$(3.11) \quad \begin{aligned} d(\eta_u^{n+1} - \eta_u^n, q) + c(\eta_p^{n+1} - \eta_p^n, q) + \tau b(u^{n+1}; \eta_p^{n+1}, q) \\ &= d(\bar{u}^{n+1} - \bar{u}^n - \tau D_\tau u^{n+1}, q) + c(\bar{p}^{n+1} - \bar{p}^n - \tau D_\tau p^{n+1}, q) + \tau b(u^{n+1}; \eta_p^{n+1}, q) \\ &= d(\theta_u^{n+1}, q) + c(\theta_p^{n+1}, q) + \tau [b(u^{n+1}; \bar{p}^{n+1}, q) - b(\bar{u}^{n+1}; \bar{p}^{n+1}, q)] \end{aligned}$$

for all $q \in \mathcal{Q}$. Summing up (3.9) and (3.11) for the particular choices $v = \eta_u^{n+1} - \eta_u^n$ and $q = \eta_p^{n+1}$, we obtain

$$(3.12) \quad \begin{aligned} a(\eta_u^{n+1}, \eta_u^{n+1} - \eta_u^n) + c(\eta_p^{n+1}, \eta_p^{n+1} - \eta_p^n) + \tau b(u^{n+1}; \eta_p^{n+1}, \eta_p^{n+1}) \\ &= -d(\eta_u^{n+1} - \eta_u^n, \eta_p^{n+1} - \eta_p^n) + d(\theta_u^{n+1}, \eta_p^{n+1}) + c(\theta_p^{n+1}, \eta_p^{n+1}) \\ &\quad + \tau [b(u^{n+1}; \bar{p}^{n+1}, \eta_p^{n+1}) - b(\bar{u}^{n+1}; \bar{p}^{n+1}, \eta_p^{n+1})]. \end{aligned}$$

In the following, we apply the identity $2a(u, u - v) = \|u\|_a^2 - \|v\|_a^2 + \|u - v\|_a^2$ and the corresponding formula for the bilinear form c . Hence, with (3.12) and Assumption 2.5 we further get

$$(3.13) \quad \begin{aligned} \|\eta_u^{n+1}\|_a^2 - \|\eta_u^n\|_a^2 + \|\tau D_\tau \eta_u^{n+1}\|_a^2 + \|\eta_p^{n+1}\|_c^2 - \|\eta_p^n\|_c^2 + \|\tau D_\tau \eta_p^{n+1}\|_c^2 + 2c_b \tau \|\eta_p^{n+1}\|_{\mathcal{Q}}^2 \\ \leq -2d(\tau D_\tau \eta_u^{n+1}, \tau D_\tau \eta_p^{n+1}) + 2d(\theta_u^{n+1}, \eta_p^{n+1}) + 2c(\theta_p^{n+1}, \eta_p^{n+1}) \\ + 2\tau [b(u^{n+1}; \bar{p}^{n+1}, \eta_p^{n+1}) - b(\bar{u}^{n+1}; \bar{p}^{n+1}, \eta_p^{n+1})]. \end{aligned}$$

Next, we consider a weighted version of Young's inequality, which gives

$$(3.14) \quad -2d(\tau D_\tau \eta_u^{n+1}, \tau D_\tau \eta_p^{n+1}) \leq \frac{C_d^2}{c_a c_c} \|\tau D_\tau \eta_u^{n+1}\|_a^2 + \|\tau D_\tau \eta_p^{n+1}\|_c^2.$$

For the second and third term on the right-hand side of (3.13) we similarly obtain

$$(3.15) \quad 2d(\theta_u^{n+1}, \eta_p^{n+1}) \leq 2\tilde{C}_d \|\theta_u^{n+1}\|_{\mathcal{H}_V} \|\eta_p^{n+1}\|_{\mathcal{Q}} \leq \frac{\tilde{C}_d^2}{c_b} \frac{4}{\tau} \|\theta_u^{n+1}\|_{\mathcal{H}_V}^2 + \frac{c_b \tau}{4} \|\eta_p^{n+1}\|_{\mathcal{Q}}^2$$

and with the continuity constant $C_{\mathcal{Q} \hookrightarrow \mathcal{H}_Q}$ of the embedding $\mathcal{Q} \hookrightarrow \mathcal{H}_Q$,

$$(3.16) \quad 2c(\theta_p^{n+1}, \eta_p^{n+1}) \leq 2C_c \|\theta_p^{n+1}\|_{\mathcal{H}_Q} \|\eta_p^{n+1}\|_{\mathcal{H}_Q} \leq \frac{C_c^2 C_{\mathcal{Q} \hookrightarrow \mathcal{H}_Q}^2}{c_b} \frac{4}{\tau} \|\theta_p^{n+1}\|_{\mathcal{H}_Q}^2 + \frac{c_b \tau}{4} \|\eta_p^{n+1}\|_{\mathcal{Q}}^2.$$

For the last term of the right-hand side in (3.13), we apply once more the weighted version of Young's inequality. This leads to the estimate

$$(3.17) \quad \begin{aligned} 2\tau [b(u^{n+1}; \bar{p}^{n+1}, \eta_p^{n+1}) - b(\bar{u}^{n+1}; \bar{p}^{n+1}, \eta_p^{n+1})] &\leq 2\tau L_b \|\bar{p}^{n+1}\|_{\mathcal{Q}} \|\eta_p^{n+1}\|_{\mathcal{Q}} \|\eta_u^{n+1}\|_V \\ &\leq \frac{c_b \tau}{2} \|\eta_p^{n+1}\|_{\mathcal{Q}}^2 + \frac{2\tau L_b^2}{c_a c_b} \|\bar{p}^{n+1}\|_{\mathcal{Q}}^2 \|\eta_u^{n+1}\|_a^2. \end{aligned}$$

We now combine the estimates (3.13)–(3.17) and absorb the terms $\|\tau D_\tau \eta_p^{n+1}\|_c^2$, $\tau \|\eta_p^{n+1}\|_b$, and $\|\tau D_\tau \eta_u^{n+1}\|_a^2$. For the latter, we use Assumption 2.3. In total, this yields

$$\begin{aligned} \|\eta_u^{n+1}\|_a^2 - \|\eta_u^n\|_a^2 + \|\eta_p^{n+1}\|_c^2 - \|\eta_p^n\|_c^2 + c_b \tau \|\eta_p^{n+1}\|_{\mathcal{Q}}^2 \\ \leq \tau \frac{2L_b^2}{c_a c_b} \|\bar{p}^{n+1}\|_{\mathcal{Q}}^2 \|\eta_u^{n+1}\|_a^2 + \frac{4}{c_b \tau} \left(\tilde{C}_d^2 \|\theta_u^{n+1}\|_{\mathcal{H}_V}^2 + C_c^2 C_{\mathcal{Q} \hookrightarrow \mathcal{H}_Q}^2 \|\theta_p^{n+1}\|_{\mathcal{H}_Q}^2 \right). \end{aligned}$$

Applying the *mean value theorem*, we estimate

$$\|\theta_u^{n+1}\|_{\mathcal{H}_V} \leq \tau^2 \|\ddot{u}\|_{L^\infty(\mathcal{H}_V)} \quad \text{and} \quad \|\theta_p^{n+1}\|_{\mathcal{H}_Q} \leq \tau^2 \|\ddot{p}\|_{L^\infty(\mathcal{H}_Q)}.$$

Hence, we obtain

$$(3.18) \quad \|\eta_u^{n+1}\|_a^2 - \|\eta_u^n\|_a^2 + \|\eta_p^{n+1}\|_c^2 - \|\eta_p^n\|_c^2 + c_b \tau \|\eta_p^{n+1}\|_{\mathcal{Q}}^2 \leq \tau C_1 \|\eta_u^{n+1}\|_a^2 + \tau^3 C_2$$

with constants

$$C_1 := \frac{2L_b^2}{c_a c_b} \|\bar{p}\|_{L^\infty(\mathcal{Q})}^2 \quad \text{and} \quad C_2 := \frac{4}{c_b} \tilde{C}_d^2 \|\ddot{u}\|_{L^\infty(\mathcal{H}_V)} + \frac{4}{c_b} C_c^2 C_{\mathcal{Q} \hookrightarrow \mathcal{H}_Q}^2 \|\ddot{p}\|_{L^\infty(\mathcal{H}_Q)}.$$

Due to the assumption on the step size (3.8), which now reads $\tau C_1 < 1$, we can apply a discrete Grönwall inequality to (3.18), see [Emm99, Prop. 3.1]. This yields

$$\|\eta_u^n\|_a^2 + \|\eta_p^n\|_c^2 \leq \tau^2 \frac{C_2}{C_1} (\exp(C_1 t_n) - 1).$$

On the other hand, the summation of (3.18) over n (using $\eta_u^0 = 0$ and $\eta_p^0 = 0$) and using the previous estimate yields

$$(3.19) \quad c_b \tau \sum_{k=1}^n \|\eta_p^k\|_{\mathcal{Q}}^2 \leq \tau C_1 \sum_{k=1}^n \|\eta_u^k\|_a^2 + \tau^2 t_n C_2 \leq \tau^2 t_n C_2 \exp(C_1 t_n)$$

and hence the assertion. \square

3.4. Summary and main result. For the main result, which states first-order convergence of the semi-explicit method for poroelasticity with nonlinear permeability, we combine the two previous propositions. This then leads to the following statement.

Theorem 3.7 (Convergence of the semi-explicit scheme). *Consider the setting of Section 2.1 with b defined in (2.3) as well as Assumptions 2.3, 2.5, and 3.3. Let (u, p) denote the exact solution to (2.4) with $p(0) = p^0 \in \mathcal{Q}$ and (u^n, p^n) the sequence resulting from (3.3) for $n \leq T/\tau$ with the same initial data. If the step size satisfies the restriction (3.8), then there exists a constant C (depending on p and \bar{p}) such that*

$$\|u(t_n) - u^n\|_{\mathcal{V}}^2 + \|p(t_n) - p^n\|_{\mathcal{H}_{\mathcal{Q}}}^2 \lesssim \tau^2 (1 + t_n) \exp(C t_n).$$

Proof. One can easily define a history function satisfying (3.5). The assertion directly follows from the two previous Propositions 3.4 and 3.5 and the triangle inequality. \square

Recall that we have no pointwise estimates of the pressure variable in the \mathcal{Q} -norm. To get an estimate in $L^2(0, T; \mathcal{Q})$, let us define the piecewise constant function $P \in L^2(0, T; \mathcal{Q})$ by

$$P(0) := p^0, \quad P(t) := p^k \text{ for } t \in (t_{k-1}, t_k].$$

Then the combination of Propositions 3.4 and 3.5 shows

$$\|p - P\|_{L^2(0, t_n; \mathcal{Q})}^2 = \int_0^{t_n} \|p(t) - P(t)\|_{\mathcal{Q}}^2 dt \lesssim \tau^2 (1 + t_n) \exp(C t_n).$$

Remark 3.8 (spatial discretization). For practical computations, one would consider discrete spaces $V_h \subseteq \mathcal{V}$ and $Q_h \subseteq \mathcal{Q}$, leading to approximations $u_h^n \approx u(t_n)$ and $p_h^n \approx p(t_n)$. Then, a similar convergence result can be shown based on spatial projections corresponding to a and b , namely $R_a: \mathcal{V} \rightarrow V_h$ and (for a fixed $w \in \mathcal{V}$) $R_b^w: \mathcal{Q} \rightarrow Q_h$, defined by

$$a(R_a u, v_h) = a(u, v_h), \quad b(w; R_b^w p, q_h) = b(w; p, q_h)$$

for all $v_h \in V_h$, $q_h \in Q_h$. Assuming approximation properties

$$\|u - R_a u\|_{\mathcal{H}_{\mathcal{V}}} \lesssim h \|u\|_{\mathcal{V}}, \quad \|u - R_a u\|_{\mathcal{V}} \lesssim h \|\nabla^2 u\|_{\mathcal{H}_{\mathcal{V}}}$$

and

$$\|p - R_b^w p\|_{\mathcal{H}_{\mathcal{Q}}} \lesssim h \|p\|_{\mathcal{Q}}, \quad \|p - R_b^w p\|_{\mathcal{Q}} \lesssim h \|\nabla^2 p\|_{\mathcal{H}_{\mathcal{Q}}}, \quad \|p - R_b^w p\|_{\mathcal{H}_{\mathcal{Q}}} \lesssim h^2 \|\nabla^2 p\|_{\mathcal{H}_{\mathcal{Q}}},$$

uniformly in w , we obtain an error estimate of the form

$$\|u(t_n) - u_h^n\|_a^2 + \|p(t_n) - p_h^n\|_c^2 \lesssim (\tau^2 + h^2 + h^4/\tau) \exp(C t_n).$$

Hence, in the (not critical) regime $h^2 \lesssim \tau$ we have first-order convergence in τ and h .

Closing this section, we would like to emphasize that the presented convergence theory remains valid for a non-vanishing right-hand side in (2.1a), introducing volume-distributed external forces. We now turn to the numerical investigation of the semi-explicit scheme, considering three test cases.

4. NUMERICAL EXAMPLES

Besides the numerical validation of the obtained convergence rates, this section is devoted to the following questions:

- performance of the semi-explicit scheme compared to implicit schemes,
- necessity of the weak coupling condition given in Assumption 2.3,
- convergence for more general right-hand sides.

All computations are based on a finite element implementation in Python based on the computing platform *FEniCS*. Throughout this section, h denotes the spatial discretization parameter that corresponds to a classical first-order finite element approximation on a regular mesh. Moreover, we use equidistant time steps as mentioned in Section 3.

4.1. Network-inspired model. In this first example, we use the network-inspired porosity-permeability relation as presented in Example 2.9 with

$$\kappa_0 = 1.307 \cdot 10^3, \quad \rho_0 = 0.4, \quad \hat{\rho} = 0.2, \quad \delta = 0.01.$$

As computational domain we consider the unit square $D = (0, 1)^2$. Inspired by the examples in [RLVM20], we further choose the remaining parameters as

$$\lambda = 2.019 \cdot 10^7, \quad \mu = 1.346 \cdot 10^7, \quad \alpha = 0.8, \quad M = 10, \quad \nu = 10^{-6}, \quad T = 1.$$

The right-hand side g and the initial condition p^0 are given by

$$\begin{aligned} g(x, t) &= 30 \sin(\pi x_1) \exp(-t), \\ p^0(x) &= 50(1 - x_1)x_1(1 - x_2)x_2. \end{aligned}$$

We emphasize that the coupling condition from Assumption 2.3 is fulfilled for this setup, since $C_d^2 = \alpha^2 = 0.64$ and $c_a c_c \approx \mu/M = 1.346 \cdot 10^6$.

To investigate the performance of the semi-explicit scheme, we compare the results for multiple mesh sizes h and time step sizes τ with a reference solution computed with $h_{\text{ref}} = \tau_{\text{ref}} = 2^{-8}$ and the implicit scheme (3.2), where the inner iteration is handled with a Picard-type approach. The inner iteration stops when a relative residual error of 10^{-9} is reached. For this model, we have observed that at most three Picard steps were needed to converge for each point in time.

For a numerical comparison, we also present the approximations for different discretization parameters with an implicit approach coupled with an inner Picard iteration as for the reference solution. The stopping criterion for the inner iteration is a relative residual error of 10^{-9} and as for the reference solution at most three Picard steps were needed to reach this threshold. We present the errors at the final point in time $t = T = t_N$ measured in the norms $\|\cdot\|_a$ (equivalent to the \mathcal{V} -norm) and $\|\cdot\|_c$ (equivalent to the \mathcal{H}_Q -norm) for the variables u and p , respectively. For further investigations, we also show errors measured in the norms $\|\cdot\|_{\mathcal{H}_V}$ (for u) and $\|\cdot\|_{\mathcal{Q}}$ (for p).

In Figure 4.1, the mesh size $h = 2^{-7}$ is chosen such that the temporal error dominates. Based on the above theory, we expect linear convergence in τ for the semi-explicit scheme. This is observed for both variables p and u and the errors are very close to the errors of the implicit scheme combined with a Picard iteration, especially for the variable p , since the coupling is very weak in this particular example. The slight stagnation in Figure 4.1 for both curves can be explained by the spatial error that dominates for smaller values of τ . Let us also mention that the errors in the \mathcal{H}_V -norm (for u) and the \mathcal{Q} -norm (for p) show a linear behavior in τ as well.

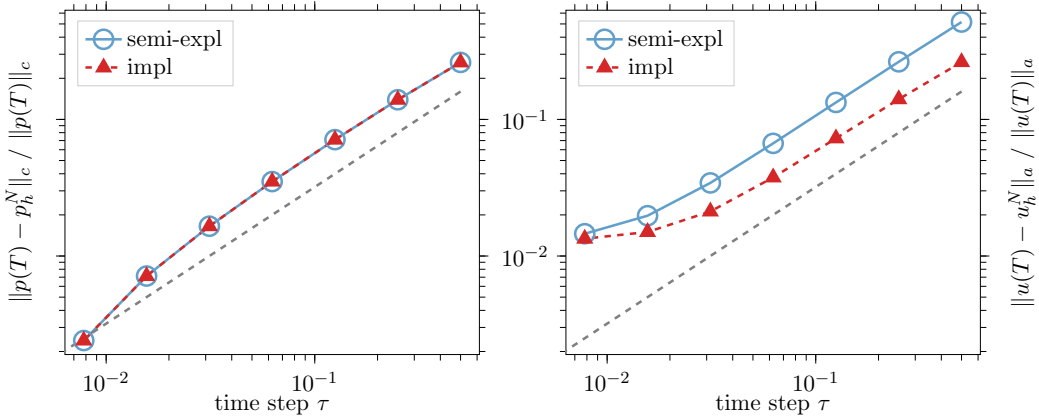


FIGURE 4.1. Relative error in p (left, measured in the c -norm) and u (right, a -norm) at the final time T for fixed $h = 2^{-7}$ and varying τ . The dashed line indicates order 1.

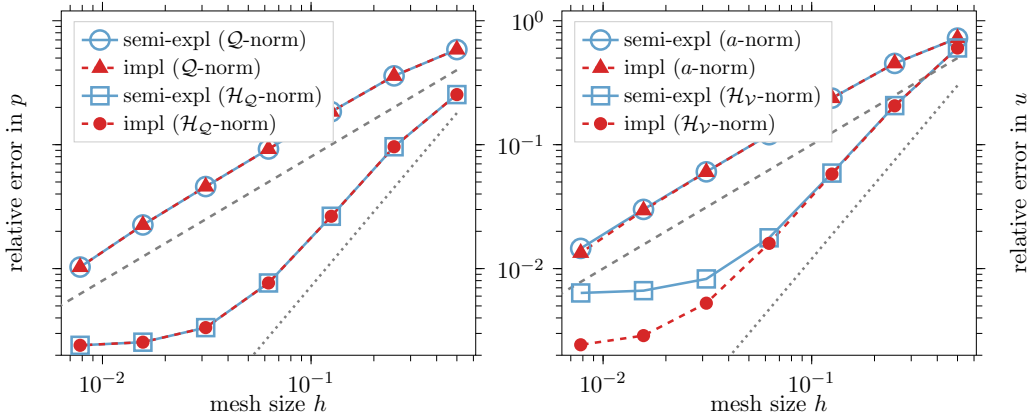


FIGURE 4.2. Relative error in p (left, measured in the Q and \mathcal{H}_Q -norm) and u (right, a and \mathcal{H}_V -norm) at the final time T for fixed $\tau = 2^{-7}$ and varying h . The dashed and the dotted lines indicate orders 1 and 2, respectively.

Although we are mainly interested in the temporal error, for completeness we also present the spatial errors in Figure 4.2 for a fixed time step size $\tau = 2^{-7}$. We observe first-order rates for both schemes in u and p when measured in the H^1 -norms. For the weaker L^2 -norms, the plots indicate second order convergence with a commencing stagnation when the temporal error dominates. This is in line with classical approximation results of first-order finite element approximations.

4.2. Sharpness of the coupling condition. This subsection is devoted to showing that the weak coupling condition in Assumption 2.3 is indeed necessary and rather sharp. For this, we analyze a purely academic example that is based on [AMU21b] and only involves temporal dependencies. More precisely, we take $\mathcal{V} = \mathcal{H}_V := \mathbb{R}^3$, $\mathcal{Q} = \mathcal{H}_Q := \mathbb{R}$ and the

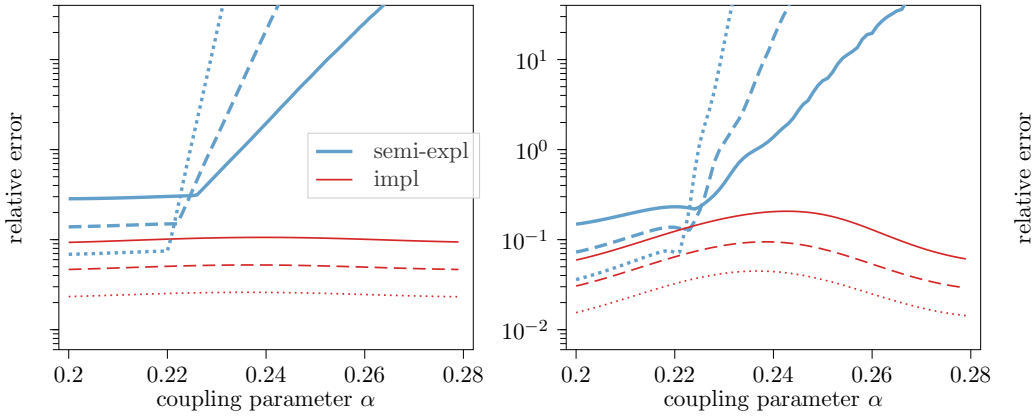


FIGURE 4.3. Illustration of the practical coupling condition for the nonlinearity κ with constant $k = 1$ (left) and $k = 10$ (right). The step sizes are given by $\tau = 2^{-4}$ (solid line), $\tau = 2^{-5}$ (dashed line), and $\tau = 2^{-6}$ (dotted line). Plots contain the relative error at the end of the time interval, i.e., $\|p(T) - p_N\|/\|p(T)\| + \|u(T) - u_N\|/\|u(T)\|$.

bilinear forms

$$a(u, v) := v^T A u, \quad d(v, p) := \alpha p^T D v, \quad c(p, q) := q^T p, \quad b(u; p, q) := \kappa(u) q^T p$$

with $\alpha \geq 0$ and the matrices

$$A := \begin{bmatrix} 2 & -1 & 0 \\ -1 & 2 & -1 \\ 0 & -1 & 2 \end{bmatrix}, \quad D := \begin{bmatrix} 1 & 2 & 3 \end{bmatrix}.$$

The nonlinearity κ is defined by

$$\kappa(u) := \frac{1}{100} + \frac{k}{10} \cos(\pi(u_1 + u_2 + u_3))^2$$

with a given constant $k > 0$ tuning the nonlinearity. Besides, we have the right-hand side

$$g(t) := \frac{1 + 21\alpha^2}{2} \pi \cos(\frac{1}{2}\pi t) + \kappa(u(t)) p(t),$$

which yields as exact solution

$$p(t) = \sin(\frac{\pi}{2}t), \quad u(t) = \frac{\alpha}{2} [5 \ 8 \ 7]^T \sin(\frac{\pi}{2}t).$$

In Figure 4.3, we present the resulting errors of the implicit and the semi-explicit discretization for different time step sizes $\tau \in \{2^{-4}, 2^{-5}, 2^{-6}\}$, multiple coefficients $\alpha \in [0.2, 0.25]$, and constants $k \in \{1, 10\}$.

We observe that for all three time step sizes, the deterioration starts for $\alpha \approx 0.22$. The weak coupling condition in Assumption 2.3 demands $\alpha \leq 0.205$ since $c_c = 1$, $c_a \approx 0.586$ and $C_d \approx 3.742\alpha$. This is as well in line with the findings for the linear setting in [AMU21a], where the coupling condition can be slightly relaxed compared to the theory. As expected, the implicit scheme is unconditionally stable. Finally, we emphasize that the critical point is not affected by the bounds of κ (cf. Remark 2.7). In this particular example, we have $\kappa_+ = 0.11$ in the left plot and $\kappa_+ = 1.01$ in the right one.

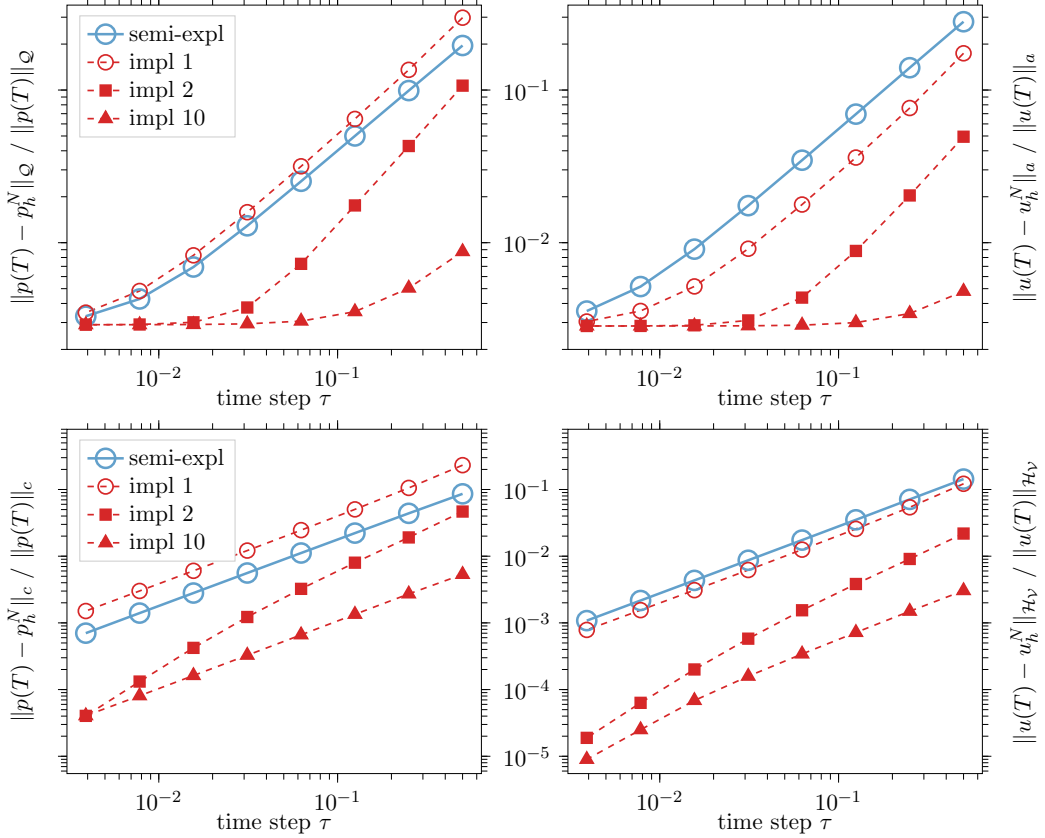


FIGURE 4.4. Relative H^1 -errors (top) and L^2 -errors (bottom) at final time T for the semi-explicit method and implicit approximations with different maximal Picard steps with fixed parameter $h = 2^{-8}$ and varying τ .

4.3. Kozeny-Carman model. For our third and final example, we consider a Kozeny-Carman permeability as explained in Example 2.8 and go beyond the above theory by also considering a non-zero right-hand side f in (2.1a). We set the involved coefficients as

$$\rho_0 = 0.5, \quad c_s = -0.75, \quad C_s = 0.75, \quad \alpha = \lambda = \mu = \kappa_0 = \nu = M = T = 1.$$

The right-hand sides f , g and the initial data p^0 are chosen such that

$$p(x, t) = t \sin(\pi x_1) \sin(\pi x_2), \quad u(x, t) = \frac{1}{6} [1 \ 1]^T \exp(-t) \sin(\pi x_1) \sin(\pi x_2)$$

is the corresponding exact solution. In this case, we have $C_d^2 = \alpha^2 = 1$ and $c_a c_c \approx \mu/M = 1$. Hence, this model represents the critical regime of the weak coupling condition of Assumption 2.3.

This setup is taken from the example considered in [CCM13], where only an implicit scheme in combination with a Picard-type iteration is used. Here, we compare our semi-explicit approach with three different implicit approaches, where either maximal one, two, or ten Picard iterations are performed for each time step. This means, the iteration either stops after the maximal amount of steps or when the relative residual tolerance of 10^{-9} is reached. Using the norms $\|\cdot\|_a$ and $\|\cdot\|_Q$ for the variables u and p , respectively, we

TABLE 4.1. Run time comparison (in seconds) for fixed $h = 2^{-8}$

τ	2^{-4}	2^{-5}	2^{-6}	2^{-7}	2^{-8}
semi-explicit	245	473	951	1923	3733
implicit (max. 10 Picard steps)	5323	10075	17958	31176	40371
speed-up factor	21.7	21.3	18.9	16.2	10.8
implicit (max. 2 Picard steps)	1327	2611	5428	10718	16456
speed-up factor	5.4	5.5	5.7	5.6	4.4
implicit (max. 1 Picard steps)	755	1502	3008	6100	11256
speed-up factor	3.1	3.1	3.2	3.2	3.0

present in Figure 4.4 (top) the relative errors for these four methods and different values of τ for a fixed mesh size $h = 2^{-8}$. We observe a linear convergence behavior in τ for both u and p , but the curves stagnate when the spatial error starts to dominate. The level of stagnation is similar for all curves due to the fact that the spatial errors behave similarly for these approaches as already observed in the first example (cf. Figure 4.2). Note that the semi-explicit scheme is closest to the implicit approximation with just one Picard step.

Apart from the behavior with respect to these stronger norms, we also present the errors in the \mathcal{H}_V -norm and \mathcal{H}_Q -norm, respectively (Figure 4.4 (bottom)). Due to the smaller spatial error in these weaker norms, the error curves do not show a stagnation and display a linear convergence behavior in τ .

Additionally to the convergence rate, another important aspect with the semi-explicit approach is the speed-up due to the decoupling and the automatic linearization. To this end, we compare the run times of the semi-explicit scheme with the ones of the implicit Picard-type approaches with maximal one, two, or ten inner iteration steps. We emphasize that, although the errors of the semi-explicit method and the implicit one with just one Picard step are close, the speed-up of the semi-explicit scheme is at least with factor three, cf. Table 4.1. Although it is even better compared to the other implicit schemes, one has to keep in mind that the error values are also lower for these schemes.

4.4. Discussion of results. In view of the results of the previous subsections, we can first record that for a coupling between the two poroelastic equations that is relatively weak (i.e., the coupling condition in Assumption 2.3 is not critical at all), the semi-explicit scheme not only provides similar results as the implicit ones but also leads to much faster computations. Only the constant in the temporal error estimate seems to be slightly larger than the corresponding constant for the implicit schemes, which explains the differences in the plots in Section 4.1.

For a coupling behavior that is rather sharp with respect to the coupling condition in Assumption 2.3, one still observes a significant speed-up with the semi-explicit scheme, especially if multiple Picard iteration steps are necessary for the implicit discretization. However, this comes at the cost of larger errors. In such a setting, the speed-up does merely outweigh the demand of smaller time steps in order to achieve an error below some prescribed tolerance.

Finally, we mention that the coupling condition in Assumption 2.3 is indeed necessary when using the semi-explicit scheme as investigated in Section 4.2. It can be, however, slightly relaxed in practical experiments compared to the theoretical assumption.

5. CONCLUSIONS

Within this paper, we have proposed the use of a semi-explicit discretization scheme for the problem of nonlinear poroelasticity with displacement-dependent permeability. In the setting of a weak coupling of the two involved equations, the scheme allows a decoupling and, in particular, results directly in a one-step linearization approach to treat the nonlinearity. We proved first-order convergence in time and illustrated the performance of the approach in multiple numerical examples. The semi-explicit method provides a significant speed-up compared to a classical implicit scheme with an inner iteration, especially for a relatively weak coupling of the equations.

ACKNOWLEDGMENTS

R. Maier gratefully acknowledges support by the Göran Gustafsson Foundation for Research in Natural Sciences and Medicine.

REFERENCES

- [ACM⁺20] R. Altmann, E. Chung, R. Maier, D. Peterseim, and S.-M. Pun. Computational multiscale methods for linear heterogeneous poroelasticity. *J. Comput. Math.*, 38(1):41–57, 2020.
- [AMU20] R. Altmann, V. Mehrmann, and B. Unger. Port-Hamiltonian formulations of poroelastic network models. *ArXiv Preprint*, (2012.01949), 2020.
- [AMU21a] R. Altmann, R. Maier, and B. Unger. Semi-explicit discretization schemes for weakly-coupled elliptic-parabolic problems. *Math. Comp.*, 90:1089–1118, 2021.
- [AMU21b] R. Altmann, R. Maier, and B. Unger. A semi-explicit integration scheme for weakly-coupled poroelasticity with nonlinear permeability. *PAMM*, 20(1):e202000061, 2021.
- [Bal87] I. Balberg. Recent developments in continuum percolation. *Philos. Mag. B*, 56(6):991–1003, 1987.
- [BGSW16] L. Bociu, G. Guidoboni, R. Sacco, and J. T. Webster. Analysis of nonlinear poro-elastic and poro-visco-elastic models. *Arch. Rational Mech. Anal.*, 222(3):1445–1519, 2016.
- [Bio41] M. A. Biot. General theory of three-dimensional consolidation. *J. Appl. Phys.*, 12(2):155–164, 1941.
- [Bio56] M. A. Biot. Thermoelasticity and irreversible thermodynamics. *J. Appl. Phys.*, 27:240–253, 1956.
- [BRKN18] M. Borregales, F. A. Radu, K. Kumar, and J. M. Nordbotten. Robust iterative schemes for non-linear poromechanics. *Comput. Geosci.*, 22(4):1021–1038, 2018.
- [BV16] D. L. Brown and M. Vasilyeva. A generalized multiscale finite element method for poroelasticity problems II: Nonlinear coupling. *J. Comput. Appl. Math.*, 297:132–146, 2016.
- [BZ03] A. Bellen and M. Zennaro. *Numerical Methods for Delay Differential Equations*. Oxford University Press, New York, 2003.
- [Car37] P. C. Carman. Fluid flow through granular beds. *Trans. Inst. Chem. Eng.*, 15:150–166, 1937.
- [Car38] P. C. Carman. Determination of the specific surface of powders i. transactions. *J. Soc. Chem. Indus.*, 57:225–234, 1938.
- [CCM13] Y. Cao, S. Chen, and A. J. Meir. Analysis and numerical approximations of equations of nonlinear poroelasticity. *Discrete Cont. Dyn.-B*, 18(5), 2013.
- [CGH⁺14] P. Causin, G. Guidoboni, A. Harris, D. Prada, R. Sacco, and S. Terragni. A poroelastic model for the perfusion of the lamina cribrosa in the optic nerve head. *Math. Biosci.*, 257:33–41, 2014.
- [Cia88] P. G. Ciarlet. *Mathematical elasticity. Vol. I*. North-Holland, Amsterdam, 1988.
- [CR14] W. D. Callister and D. G. Rethwisch. *Materials science and engineering: An introduction*. Wiley, Hoboken, NJ, ninth edition, 2014.

[DC93] E. Detournay and A. H. D. Cheng. Fundamentals of poroelasticity. In *Analysis and design methods*, pages 113–171. Elsevier, 1993.

[EM09] A. Ern and S. Meunier. A posteriori error analysis of Euler-Galerkin approximations to coupled elliptic-parabolic problems. *ESAIM: Math. Model. Numer. Anal.*, 43(2):353–375, 2009.

[Emm99] E. Emmrich. Discrete versions of Gronwall's lemma and their application to the numerical analysis of parabolic problems. *Fachbereich Mathematik, TU Berlin*, Preprint No. 637, 1999.

[Eva98] L. C. Evans. *Partial Differential Equations*. American Mathematical Society (AMS), Providence, second edition, 1998.

[FAC⁺19] S. Fu, R. Altmann, E. Chung, R. Maier, D. Peterseim, and S.-M. Pun. Computational multiscale methods for linear poroelasticity with high contrast. *J. Comput. Phys.*, 395:286–297, 2019.

[FCM20] S. Fu, E. Chung, and T. Mai. Constraint energy minimizing generalized multiscale finite element method for nonlinear poroelasticity and elasticity. *J. Comput. Phys.*, 417:109569, 2020.

[HC90] C.-T. Hsu and P. Cheng. Thermal dispersion in a porous medium. *Int. J. Heat Mass Tran.*, 33(8):1587–1597, 1990.

[HM90] M. H. Holmes and V. C. Mow. The nonlinear characteristics of soft gels and hydrated connective tissues in ultrafiltration. *J. Biomech.*, 23(11):1145–1156, 1990.

[Koz27] J. Kozeny. Über kapillare Leitung des Wassers im Boden. *Royal Academy of Science, Vienna, Proc. Class I*, 136:271–306, 1927.

[KP99] J.-M. Kim and R. R. Parizek. A mathematical model for the hydraulic properties of deforming porous media. *Groundwater*, 37(4):546–554, 1999.

[KTJ11] J. Kim, H. A. Tchelepi, and R. Juanes. Stability and convergence of sequential methods for coupled flow and geomechanics: fixed-stress and fixed-strain splits. *Comput. Methods Appl. Mech. Engrg.*, 200(13–16):1591–1606, 2011.

[LM72] J.-L. Lions and E. Magenes. *Non-homogeneous Boundary Value Problems and Applications. Vol. I*. Springer-Verlag, New York-Heidelberg, 1972.

[LM80] W. M. Lai and V. C. Mow. Drag-induced compression of articular cartilage during a permeation experiment. *Biorheology*, 17(1–2):111–123, 1980.

[MW13] A. Mikelić and M. F. Wheeler. Convergence of iterative coupling for coupled flow and geomechanics. *Comput. Geosci.*, 17(3):455–461, 2013.

[RLVM20] M. Rahrah, L. A. Lopez-Peña, F. Vermolen, and B. Meulenbroek. Network-inspired versus Kozeny–Carman based permeability-porosity relations applied to Biot's poroelasticity model. *J. Math. Industry*, 10(19), 2020.

[SBK⁺19] E. Storvik, J. W. Both, K. Kumar, J. M. Nordbotten, and F. A. Radu. On the optimization of the fixed-stress splitting for Biot's equations. *Int. J. Numer. Meth. Eng.*, 120(2):179–194, 2019.

[SEWC12] I. Sobey, A. Eisenträger, B. Wirth, and M. Czosnyka. Simulation of cerebral infusion tests using a poroelastic model. *Int. J. Numer. Anal. Model. Series B*, 3(1):52–64, 2012.

[Sho00] R. E. Showalter. Diffusion in poro-elastic media. *J. Math. Anal. Appl.*, 251(1):310–340, 2000.

[VCT⁺16] J. C. Vardakas, D. Chou, B. J. Tully, C. C. Hung, T. H. Lee, P. H. Tsui, and Y. Ventikos. Investigating cerebral oedema using poroelasticity. *Med. Eng. Phys.*, 38(1):48–57, 2016.

[WG07] M. F. Wheeler and X. Gai. Iteratively coupled mixed and Galerkin finite element methods for poro-elasticity. *Numer. Meth. Part. D. E.*, 23(4):785–797, 2007.

[Wlo92] J. Wloka. *Partial Differential Equations*. Cambridge University Press, Cambridge, 1992.

[Won88] P.-Z. Wong. The statistical physics of sedimentary rock. *Phys. Today*, 41(12):24–32, 1988.

[Zei90] E. Zeidler. *Nonlinear Functional Analysis and its Applications IIa: Linear Monotone Operators*. Springer-Verlag, New York, 1990.

[Zob10] M. D. Zoback. *Reservoir Geomechanics*. Cambridge University Press, Cambridge, 2010.

[†] DEPARTMENT OF MATHEMATICS, UNIVERSITY OF AUGSBURG, UNIVERSITÄTSSTR. 14, 86159 AUGSBURG, GERMANY

Email address: `robert.altmann@math.uni-augsburg.de`

[‡] DEPARTMENT OF MATHEMATICAL SCIENCES, CHALMERS UNIVERSITY OF TECHNOLOGY AND UNIVERSITY OF GOTHENBURG, 412 96 GÖTEBORG, SWEDEN

Email address: `roland.maier@chalmers.se`